

## Contribution to the Mapping and Geochemic Study of Geological Formations Around the Lilida Thermal Water Source (Mbongi, Ituri, Democratic Republic of Congo)

Grace Kawa, Vikandy Mambo, Désiré Kasekete, Pacifique Syakengwa, David Kaizere

kawagrace@gmail.com;

silus18@yahoo.com;

dkasekete@gmail.com;

amipacmkn@gmail.com;

fistonkaizere@gmail.com

**Keywords:** Geochemistry, Mineralization Index, Lilida Hot Spring

### ABSTRACT

The Democratic Republic of Congo, a country renowned for a geological scandal, remains virtually unexplored except for the pan-African chain flowing towards the former province of Katanga. This work remains a contribution to the geological knowledge and the discovery of the mineralization indices in the eastern part of our country, more particularly the geological formations around the thermal spring Lilida. On occasion, 8 rock samples were taken from the field. The results of X-ray geochemical lithochemical analyzes revealed that the mineral geological potential of the formations around the Lilida thermal spring of gold (Au) accompanied the complex Ag, Cd, Hg, Bi, Sn (lithophilic). The presence of tin at a remarkable content in the samples testifies that the locality of Djugu is in the context of the Mesoproterozoic where the Kibarian formations are exposed whose characteristic mineralization is tin.

### 1. INTRODUCTION

The Democratic Republic of Congo has a significant geothermal potential in the eastern part. This potentiality is closely related to the western branch of the East African Rift Valley (Esseqqat, 2011). Lilida (in Lendu dialect means hot water) is geographically located in the east of DRCONGO, Ituri province, Djugu territory, Mbongi locality at geographical coordinates 1 ° 23'44 " N and 30 ° 31 ' 23 " E. This thermal spring presents itself in a bog of mud; as a stagnant body of water gushing with low flow from a central point (Ndjele, 1988). The geological formations of the locality of Djugu are concomitant with the Kibalian formations and in close relation with the East African rift. The three major geological formations that are outcropping are: a bedrock of granitoid rocks, an amphibolite cover, and metamorphic rocks (Woodtli, 1956). This work, while remaining a contribution to the knowledge of the geology and geothermal of R.D.CONGO aims to provide new geochemical data (indices of mineralization) and geothermal Mbongi locality. More precisely, this research campaign will also make it possible to: determine the host lithology of the mineralization in the Mbongi geological formations and realize the geomorphological parameters; to provide the intellectual public with a basic document that will enable in-depth studies of the Mbongi mineralization.

### 2. LITERATURE REVIEW

The earth is active. It is characterized by tectonic movements and magmatic processes. The rise of magmas is essentially the result of plate tectonics whose movements determine three major types of boundaries and geothermal deposits: the divergent boundaries of the East African Rift case), converging boundaries, transforming boundaries (Varet, 2012. Philipe et al 2017 establish a classification to properly situate the concept of deep geothermal energy. They distinguish not only a classification based on the recoverable energy potential: very low energy (<30 ° C), low energy (between 30 ° C and 90 ° C), average energy (between 90 ° C and 150 ° C) or high energy (> 150 ° C) but also a classification according to the types of valorization of the geothermal heat: production of heat assisted by heat pump, production of heat by direct use of the geothermal heat, production of electricity. The best geothermal deposits are usually located around active volcanic areas, often near the boundaries of tectonic plates. Nearly 40 countries in the world are considered to have sufficient geothermal potential that would allow, from a more technical than economic point of view, to satisfy their entire demand for electricity by geothermal energy (Magnus et al 2012). Geothermal energy is independent of the climate and can be exploited for both heat production (house, greenhouses, fish farms and others) and electricity production (Ahmed, 2009. Omenda et al 2019 points out that in 1952 R.D.Congo was the first African country that built a geothermal micro-power plant in Kiabukwa in Katanga province. The latter gushed at a temperature of 91 ° C and produced 0.2 MW. Unfortunately this geothermal power station was abandoned a few years later.

### 3. METHODS

#### 3.1. Field work

Sampling was done on rocks in place using the geologist's hammer (Estwing USA mark). The samples were labeled and packaged in plastic bags for shipment to the testing laboratory (Brace et al, 2012). We broke the samples for which the weight was evaluated between 0.5 and 1 kg following the variation of the lithological characteristics of the ground (Brace et al, 2012, Foucault, 2014). We have georeferenced (UTM) outcrops, sampling stations, intercepts of our routes with streams, etc. using GPS (brand eTrex-10). Eight samples, chosen on the basis of lithological and lithological characteristics, were necessary for the geochemical analyzes in the BRUKER laboratory (laoratory of mines and geology at the ministry of mining in Kenya). These analyzes yielded results that were used to precisely determine the mineralization indices of geological formations around the thermal spring of Lilida. It emerges at a temperature of 36 ° C, this characteristic ranks it among the basic thermal energy sources.

### 3.2. Laboratory work

Geochemical analyzes of rock samples (NK 01-08) at the BRUKER laboratory followed the protocol of X-ray fluorescence spectrometry. The latter is a chemical analysis technique using a physical property of matter, ray fluorescence X. When material is bombarded with X-rays, the material re-emits energy in the form of, inter alia, X-rays; it is X-ray fluorescence, or X-ray secondary emission. The X-ray spectrum emitted by the material is characteristic of the composition of the sample. By analyzing this spectrum, we can deduce the elemental composition, that is to say the mass concentrations in elements. This X-ray fluorescence spectrometry is done either by wavelength dispersive analysis (WD-XRF, wavelength dispersive X-ray fluorescence spectrometry); or by dispersive energy analysis (ED-XRF, energy dispersive X-ray fluorescence spectrometry).

### 3.3. Geochemical cartographic and lithographic data processing

The field data (cartographic) were entered in Excel and transported in the QGIS software for specific treatments finally to write a sampling map. The geochemical data were processed using Excel, Past and R software, in accordance with the procedures contained in the related tutorials (Moreau, 2013, Hammer, 2017). Thus, we have elaborated the inter-element correlation matrix, constructed the content evolution curves, the regression lines, the cluster and the main component analysis (Scatter plot) diagram, as well as the standardization of the contents on the basis of their clark.

**Table 1: Clarke of the trace elements analyzed according to Foucault et al (2014) in ppm**

Element	Ag	Cd	Sn	Sb	Ba	La	Ce	Hf	Ta	W	Au	Hg	Tl	Pb	Bi	Th	U
Clarke	0,1	0,15	2	0,2	250	18	46	3	2	1,5	0,05	0,05	4500	16	0,2	9,6	2,7

Statistical studies have been useful in the clarification of inter-element enrichment or depletion in our samples. Rollinson's (1993) table showed significant correlations by interpreting the 95% confidence correlation matrix. The significant correlation corresponds to all the calculated coefficients whose absolute value is greater than or equal to the theoretical value. The degree of freedom  $Df = N - 2$  (where N is the number of samples analyzed = 8). Significant correlations have been carefully interpreted (Rollinson's Table 1993) to explain inter-element correlation.

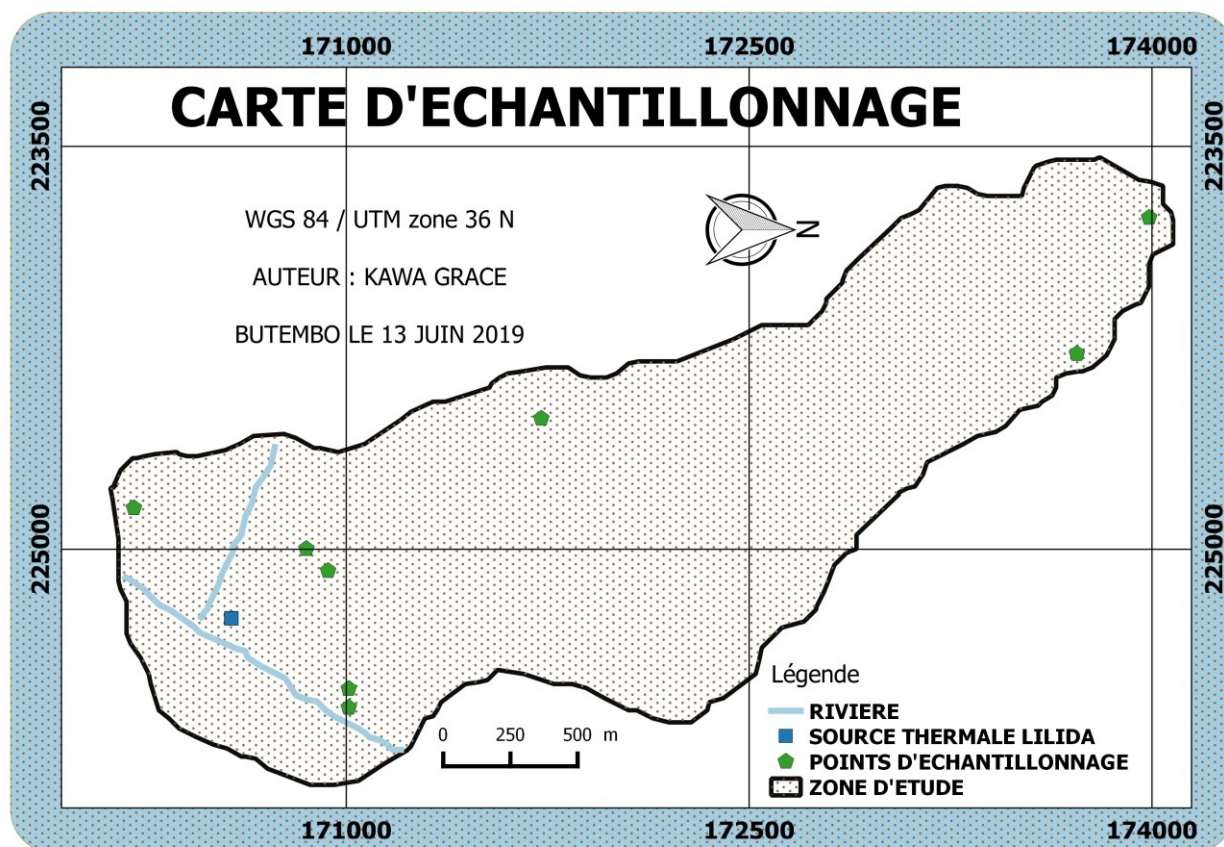


**Figure 1: sampling map**

#### 4. GEOCHEMICAL STUDY

##### 4.1. Raw results of geochemical analyzes

**Table 2 : shows the crude contents of the metal traces analyzed in the 8 samples**

ECH	Ag	Cd	Sn	Sb	Ba	La	Ce	Hf	Ta	W	Au	Hg	Tl	Pb	Bi	Th	U
NK-01	3,00	4,00	21,00	6,00	38,00	64,00	10,00	6,00	1,00	1,00	2,00	1,00	1,00	3,00	3,00	5,00	11,00
NK-02	3,00	5,00	54,00	7,00	38,00	102,00	44,00	7,00	2,00	1,00	2,00	1,00	1,00	3,00	3,00	5,00	6,00
NK-03	5,00	8,00	52,00	15,00	55,00	128,00	0,00	4,00	2,00	2,00	4,00	0,00	0,00	4,00	5,00	8,00	15,00
NK-04	3,00	4,00	64,00	10,00	36,00	73,00	0,00	6,00	2,00	1,00	2,00	1,00	1,00	2,00	3,00	5,00	9,00
NK-05	5,00	8,00	51,00	11,00	55,00	125,00	41,00	4,00	3,00	2,00	4,00	0,00	0,00	4,00	5,00	8,00	15,00
NK-06	0,00	6,00	37,00	9,00	48,00	58,00	44,00	6,00	4,00	2,00	3,00	3,00	3,00	3,00	4,00	7,00	12,00
NK-07	3,00	5,00	43,00	9,00	38,00	68,00	0,00	7,00	3,00	1,00	2,00	1,00	1,00	3,00	3,00	6,00	10,00
NK-08	3,00	5,00	39,00	6,00	38,00	94,00	0,00	6,00	2,00	1,00	2,00	1,00	1,00	3,00	3,00	5,00	10,00

##### 4.2. Statistical analysis of geochemical data

Distribution of the contents of the elements in the samples

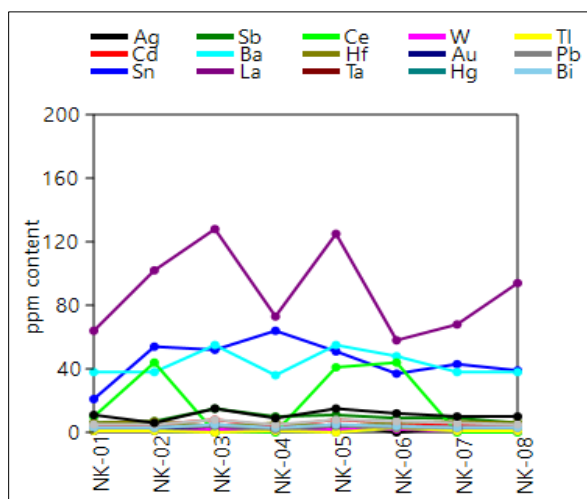


**Figure 2: Distribution of the contents of the elements in the samples**

The distribution of the contents of the trace elements in our samples is irregular. In the light of the graph of variation of the crude contents (figure 1), it appears that the lanthanum (La) is in abundance in all the samples, then the tin (Sn), the barium (Ba) and the cerium (Ce) are in profusion in the samples. Gold (Au) is present in the samples at levels between 2-4 ppm. The other metals are present in samples with low levels but not negligible.

##### Grouping the samples according to their compositional resemblance

The grouping of the samples presented in Figure 2 on the basis of geochemical analyzes reveals that there is a reconciliation of the samples which contain almost equal proportions of metals. This dendrogram presents the samples in three groups. From right to left; it is the group of samples NK (02, 03, 05) characterized by the high content of La (concentrations greater than 100 ppm); Ag, Sn, Cd Au and other metals in low concentration. The second group consists of Sample 6 which is 0 ppm Ag and enriched in Ce, Ba, Hg and other metals at non-regular concentrations. This grouping of samples is explained by the concentration of Cu and Sn. The last group is represented by NK samples (01, 08, 07 and 04). This sample assembly is motivated by the concentration of Sn, U, Hg and other metals at unequal concentrations.

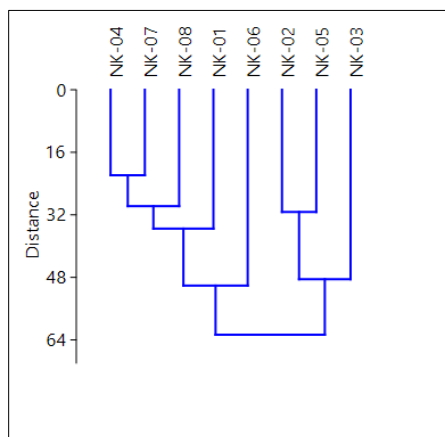


**Figure 3 : Grouping the samples according to their compositional resemblance**

This grouping of samples allowed us to identify three large groups of samples grouped according to their geochemical composition in trace metals. In order to highlight the enrichment or impoverishment of one or another element and to identify the precious element that can lead to a precise determination of the mineralization indices of the zone, it was essential to proceed to the standardization of the levels of elements in relation to their Clarke (Table 1). The table 3 aligns the standardized values of the metal traces analyzed in the 8 samples.

**Table 3 : Standardized values of element levels**

ECH	Ag	Cd	Sn	Sb	Ba	La	Ce	Hf	Ta	W	Au	Hg	Tl	Pb	Bi	Th	U
NK-01	30,00	26,67	10,50	30,00	0,15	3,56	0,25	2,00	0,50	0,67	40,00	20,00	0,00	0,19	15,00	0,52	4,07
NK-02	30,00	33,33	27,00	35,00	0,15	5,67	1,10	2,33	1,00	0,67	40,00	20,00	0,00	0,19	15,00	0,52	2,22
NK-03	50,00	53,33	26,00	75,00	0,22	7,11	0,00	1,33	1,00	1,33	80,00	0,00	0,00	0,25	25,00	0,83	5,56
NK-04	30,00	26,67	32,00	50,00	0,14	4,06	0,00	2,00	1,00	0,67	40,00	20,00	0,00	0,13	15,00	0,52	3,33
NK-05	50,00	53,33	25,50	55,00	0,22	6,94	1,03	1,33	1,50	1,33	80,00	0,00	0,00	0,25	25,00	0,83	5,56
NK-06	0,00	40,00	18,50	45,00	0,19	3,22	1,10	2,00	2,00	1,33	60,00	60,00	0,00	0,19	20,00	0,73	4,44
NK-07	30,00	33,33	21,50	45,00	0,15	3,78	0,00	2,33	1,50	0,67	40,00	20,00	0,00	0,19	15,00	0,63	3,70
NK-08	30,00	33,33	19,50	30,00	0,15	5,22	0,00	2,00	1,00	0,67	40,00	20,00	0,00	0,19	15,00	0,52	3,70

As can be read in this table 3 and in the corresponding figure 4 below, the Au, Sb, Cd, Ag metals are highly enriched in the samples at proportions of between 20-80 ppm except in the NK sample -06 where the metal Ag title 0 ppm. The latter are of a very interesting content and can be the subject of a thorough geological study. The Sn, Bi and Hg metals are present at significant levels in our samples at contents of between 10-60 ppm except in the samples NK-03 and NK-05 where the Hg contain 0 ppm. As the proportion of other metals in our samples is very low, they cannot be subject to any mining research.

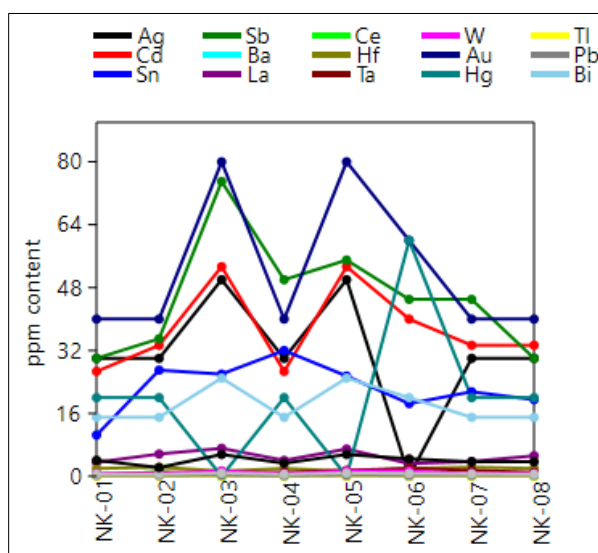


**Figure 4 : Standardized values of element levels**

#### 4.3. Principal Component Analysis (PCA) and correlation circle

This analysis consists of defining the distribution of the elements in the samples according to their influence on the construction of the axes. The examination of the factorial plots makes it possible to visualize the correlations between elements and to identify groups of samples with almost identical chemical compositions (Figure 5).

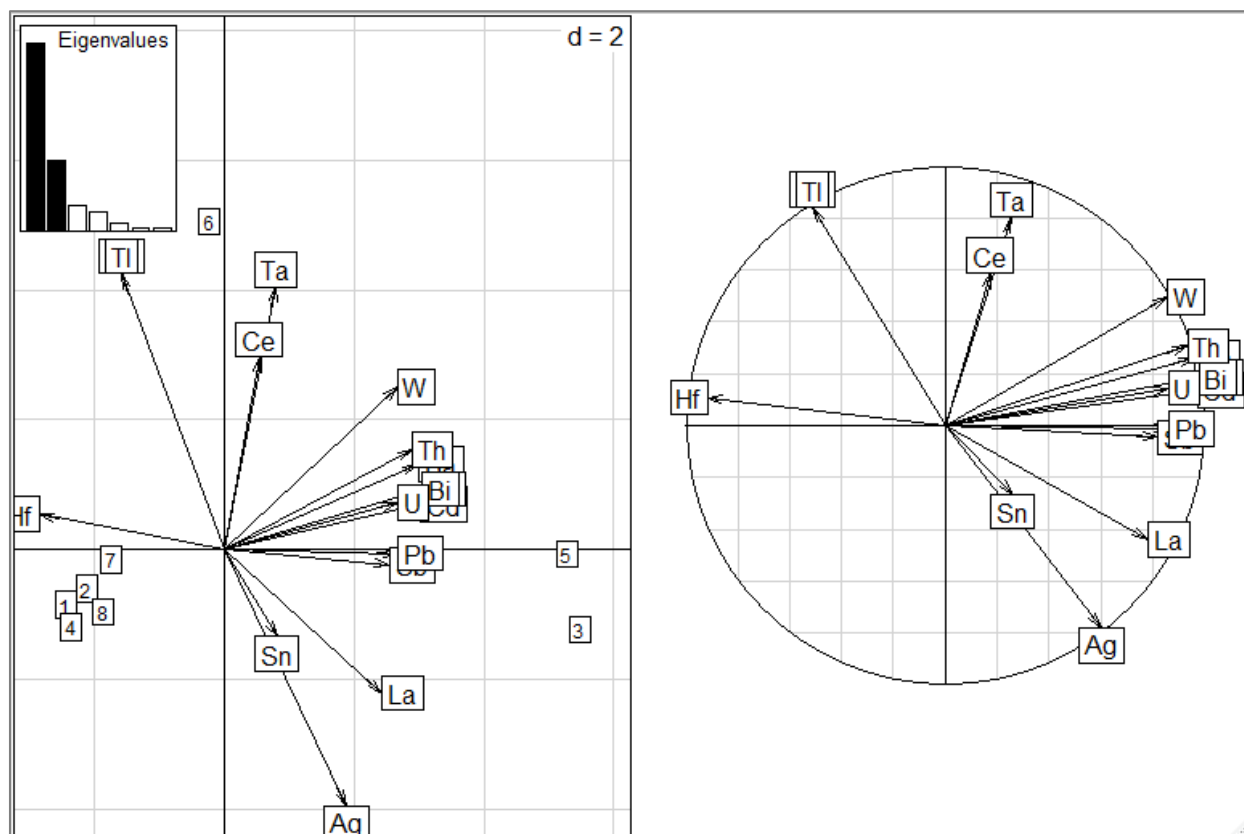


**Figure 5 : Principal Component Analysis (PCA) and correlation circle**

The principal component analysis graph (figure 4) shows that the concentrations of Cd, Sb, Ba, La, Hf, W, Au, Hg, Pb, Bi, Th, U contribute more to the formation of the factorial axis 1 which explains 59.80% of the distribution of these metal concentrations in the samples, whereas Ti, Ta, Ce, Sn, Ag, are more related to axis 2 which explains 28.73% of this distribution of elements in the samples. As for the samples, those that come closer and contribute more to the construction of the axis 1 are the samples NK (01, 02, 03, 04; 05, 07, 08) whereas the sample NK-06 contributes more to the construction of axis 2 (see Figure 9 and Annex 1). These two axes explain in total 88.53% of the distribution of the elements in the samples analyzed; the remainder of inertia is 11.47% is influenced by other geological and geochemical factors.

In fact, the principal components analysis makes it possible to apprehend the real values of the coexistence of the elements (variables) through the correlations observed during axis construction and the relationship existing between these variables and the individuals (samples) in the explanation of the phenomenon. This is to say that it summarizes the initial behavior of the elements with respect to certain membership links.

The contribution of the correlation between the geochemical parameters in the samples helps to understand certain phenomena released inter-elements and inter-samples. It gives an approach on the common origin of certain elements. It is assumed that a correlation is significant if the absolute value of the calculated correlation coefficient "r" is greater than or equal to the theoretical coefficient. The matrix (Table 5) presents the calculated values of the correlation coefficients between the different elements.

The theoretical correlation coefficient for a degree of freedom  $8 - 2 = 6$  is  $\pm 0.707$  at the 95% confidence level (see Rollinson's table, Appendix 1). From Table 5 of correlation matrix, thirty-four significant positive correlations were totalized: La-Ag, Sb-Cd, Ba-Cd, La-Cd, W-Cd, Au-Cd, Pb-Cd, Bi-Cd, Th-Cd, U-Cd, Ba-Sb, Au-Sb, Bi-Sb, Th-Sb, W-Ba, Au-Ba, Pb-Ba, Bi-Ba, Th-Ba, U-Ba, Pb-La, Bi-W, Th-W, UW, Pb-Au, Bi-Au, Th-Au, U-Au, Bi-Pb, Th-Pb, U-Pb, Th-Bi, U-Bi, U- Th and thirteen significant negative correlations Hg-Ag, Ti-Ag, Hf-Cd, Hf-Sb, Hf-Ba, Hg-La, Ti-La, W-Hf, Au-Hf, Ti-Hf, Bi-Hf, Th-Hf, U-Hf. Some linear regression lines are illustrated in Figure 6.

Table 4 : correlation matrix

Ag	1,000																	
Cd	0,482	1,000																
Sn	0,349	0,241	1,000															
Sb	0,487	<b>0,757</b>	0,526	1,000														
Ba	0,371	<b>0,966</b>	0,131	<b>0,756</b>	1,000													
La	<b>0,813</b>	<b>0,764</b>	0,460	0,562	0,638	1,000												
Ce	-0,288	0,291	0,017	-0,118	0,333	0,105	1,000											
Hf	-0,612	<b>-0,825</b>	-0,175	<b>-0,726</b>	<b>-0,868</b>	-0,705	-0,019	1,000										
Ta	-0,439	0,403	0,138	0,241	0,408	-0,125	0,485	-0,033	1,000									
W	0,111	<b>0,885</b>	0,097	0,702	<b>0,960</b>	0,442	0,422	<b>-0,770</b>	0,565	1,000								
Au	0,439	<b>0,964</b>	0,206	<b>0,800</b>	<b>0,994</b>	0,675	0,284	<b>-0,904</b>	0,362	<b>0,942</b>	1,000							
Hg	<b>-0,994</b>	-0,386	-0,341	-0,412	-0,266	<b>-0,769</b>	0,337	0,530	0,505	0,000	-0,337	1,000						
Tl	<b>-0,994</b>	-0,386	-0,341	-0,412	-0,266	<b>-0,769</b>	0,337	0,530	0,505	0,000	-0,337	<b>1,000</b>	1,000					
Pb	0,556	<b>0,889</b>	-0,104	0,511	<b>0,844</b>	<b>0,738</b>	0,245	<b>-0,718</b>	0,152	0,700	<b>0,821</b>	-0,482	-0,482	1,000				
Bi	0,439	<b>0,964</b>	0,206	<b>0,800</b>	<b>0,994</b>	0,675	0,284	<b>-0,904</b>	0,362	<b>0,942</b>	<b>1,000</b>	-0,337	-0,337	<b>0,821</b>	1,000			
Th	0,331	<b>0,948</b>	0,159	<b>0,804</b>	<b>0,970</b>	0,544	0,268	<b>-0,791</b>	0,532	<b>0,941</b>	<b>0,963</b>	-0,228	-0,228	<b>0,801</b>	<b>0,963</b>	1,000		
U	0,396	<b>0,798</b>	-0,112	0,678	<b>0,873</b>	0,433	-0,026	<b>-0,892</b>	0,258	<b>0,822</b>	<b>0,877</b>	-0,306	-0,306	<b>0,737</b>	<b>0,877</b>	<b>0,871</b>	1,000	
Ag																		
Cd																		
Sn																		
Sb																		
Ba																		
La																		
Ce																		
Hf																		
Ta																		
W																		
Au																		
Hg																		
Tl																		
Pb																		
Bi																		
Th																		
U																		

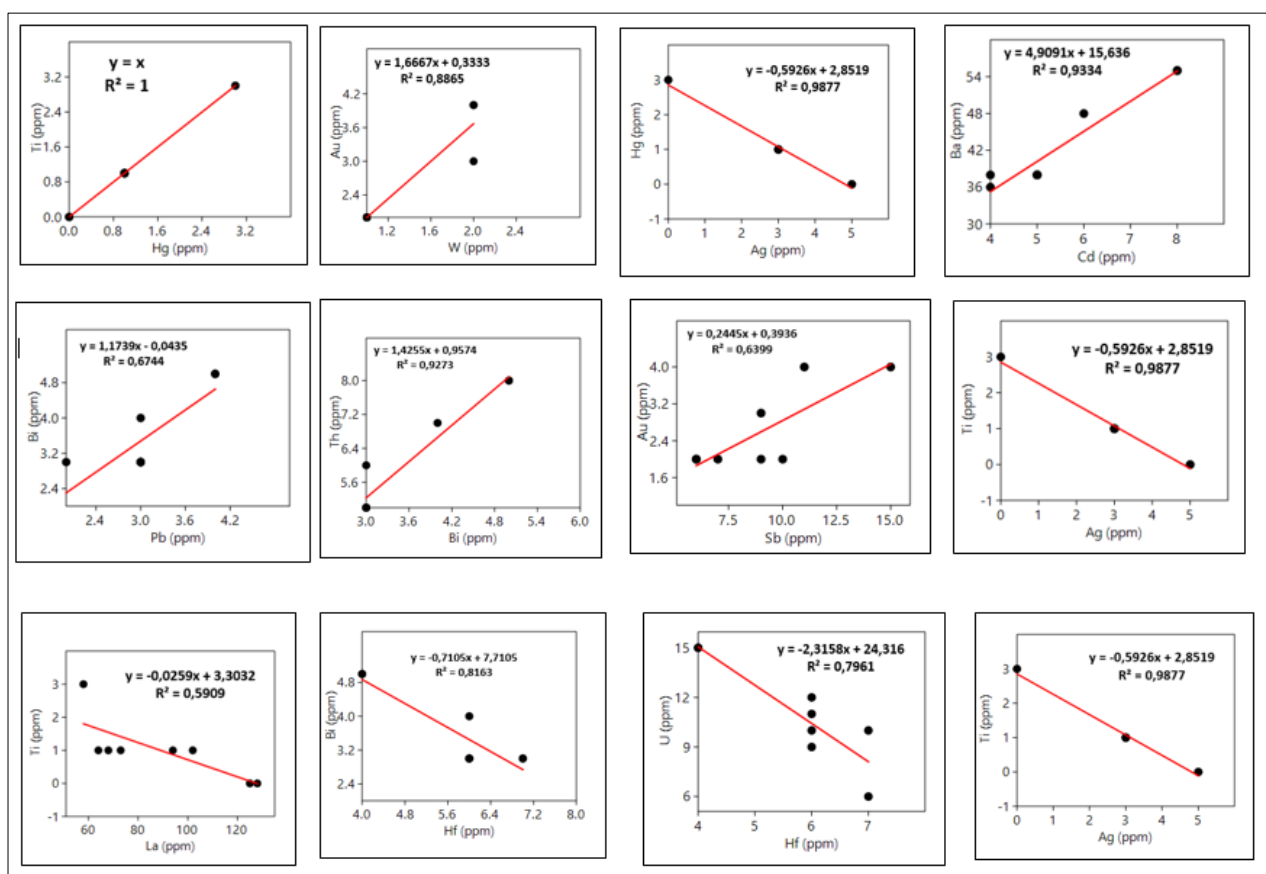


Figure 6 : regression lines

From the graphs of significant inter-element correlations (Fig. 6), we find a strong bond between Ti - Hg ( $R^2 = 1$ ); Ag - Hg ( $R^2 = 0.9877$ ); Ba-Cd ( $R^2 = 0.9334$ ); Au-W ( $R^2 = 0.8865$ ); Bi-Pb ( $R^2 = 0.6744$ ), Th-Bi ( $R^2 = 0.9273$ ), Au-Sb ( $R^2 = 0.6399$ ) while the other elements bind at correlation levels of less than 70%. It is Ti-Ag ( $R^2 = 0.9877$ ); Ti-La ( $R^2 = 0.5909$ ); Bi-Hf ( $R^2 = 0.8163$ ); U-Hf ( $R^2 = 0.7961$ ); Ti-Ag ( $R^2 = 0.9877$ ). In order to better understand these strong connections between the elements, we will try to pay particular attention to them in the discussion.



## 5. DISCUSSION

Any rock always contains a particular composition. This is clarified by the nature of the original material, the melting conditions, the crystallization and recrystallization processes, and so on. (Pomerol et al., 2006). In the locality of Djugu, around the Lilida hot spring eight samples were collected from rock and were used for geochemical analyzes. These analyzes covered seventeen elements (Ag, Cd, Sn, Sb, Ba, La, Ce, Hf, Ta, W, Au, Hg, Ti, Pb, Bi, Th, and U). Thus, after interpretation and normalization, it was found a strong enrichment in (gold) Au. In general, gold (Au) with a lighter yellow color attests the presence of silver found in nature in the native state (Schuman 1985, Bonewitz 2013, Foucault et al. Given the geological context, this type of mineralization can be classified on the one hand among the hypozonal orogenic gold (Au) deposits forming under the high metamorphic conditions ( $T > 475^{\circ}\text{C}$ ), which are very often in equilibrium with the metamorphic conditions of the country rock or which are slightly retrograde (Sylvain, 2007). In addition to the gold concentration (Au), the abundance of Ag, Cd, Hg, Bi, and Sn was found to be high in the samples compared to other analyzed elements.

From a geochemical point of view, Goldschmidt (1970) classifies Au and the complex Ag, Cd, Hg, Bi, Sn respectively among the siderophile and chalcophilic elements. It should be noted that sulphides, quartz, arsenopyrite, cobaltite, pyrite, stibine ... associate with gold (Au). Sn (tin) deposits are found throughout all geological epochs. They can be related to either the subduction zones, or the major fractures of the continental platforms, or with orogenies and the other geological formations of Kibarien. They can be associated with granites crystallizing at very different depths and in very varied geological, geochemical and structural conditions: they are found either in or around the granite domes associated with pegmatite and quartz veins (Varlamoff, 1975). The context of the Kibarian chain, this idea sticks with that announced by Rugomba et al (2010) and which states that the deposits and indices of the tin group (tin, wolframite, niobium, tantalum, beryl) are located in the part East of Congo where they form a belt extending over 700 km, from Ituri in the north to the western end of the copper belt of southern DR Congo. This is explained by the high concentration of tin and its accompanying minerals in the samples. The concentration of tin (Sn) is pinned in all our samples and thus this metal can be the subject of a systematic geological investigation since it remains one of the characteristic metals of the Kibarien (Pohl, 1992).

## 6. RECOMMENDATION AND CONCLUSION

The geochemical study done on the geological formations around the thermal spring Lilida aims to highlight the presence of potential mineralization indices in this entity. Laboratory analyzes reveal that gold Ag, Cd, Hg, Bi, Sn constitute the metallogeny of geological formations around the Lilida hot spring. This discovery in precious metals in the region is better supported by the review of literature and the geodynamic context of the area. As a reminder, the locality of Djugu is an area anchored mainly in the Kibarien basement (Lindien). This is characterized by the metamorphism of granitic rocks. Its mineralization is syngenetic and related to the emplacement of mineralized bodies, but also epigenetic associated with discontinuities caused by the tectonic jolts that affected the Kibarien. Thus, we have come to the conclusion that: the mineralization remains mainly dominated by Au Ag, Cd, Hg, Bi, Sn, the mineralization indices are syngenetic and disseminated in the surrounding rocks but also epigenetic and associated with the quartz veins.

We recommend that the Government of the Democratic Republic of Congo finance the exploration and exploitation of thermal resources on any entity of the national territory because the latter constitute a potential not studied.

## 7. REFERENCES

- Ahmed.F.A. integration of renewable energies for a sustainable policy in Djibouti. Doctoral thesis; University of Corsica. (2009).
- Bonewitz, R. L. Rocks and minerals, to recognize more than 700 rock specimens, natural guide; Larousse edition, (2013). pp. 352.
- Brace, AT. and Sheila S. I am a geologist of exploration, ed. Minerals, (2012). pp. 18.
- Essequat, H. Renewable energies in the Democratic Republic of Congo. UNEP. (2012).
- Foucault, A and Raoult, J.F. Dictionary of Geology, Dunod, Paris, (1990). pp. 355.
- Foucault, A. The amateur geologist's guide, Dunod, Paris, (2014). pp.25.
- Goldschmidt, V. M. Geochemistry. Oxford University Press, Oxford, (1970).
- Hammer, O. Reference manual of Paleontological Statistics. Ed. NHMUO, (2017). pp. 253.
- Jacques Varet; 2012. ENCYCLOPEDIA OF SUSTAINABLE DEVELOPMENT: Mineral and energy resources, energies. (2012) pp 15.
- Magnus Gehringer and Victor Loksha. Geothermal guide, planning and financing of energy production. International Bank for Reconstruction and Development. (2012) pp.170.
- Moreau, P. Excel 2013 Advanced: Training Guide with Case Studies. Ed. T Soft and Groupe Eryolles, (2013). pp. 25.
- Njele, M.-B. Phytogeographic elements endemic in the vascular flora of Zaire. PhD thesis: Université Libre de Bruxelles, (1998) pp. 528.
- Omenda, P. Geology and geothermal activity of the East African Rift. Present on IX in the short term during geothermal resource exploration: organized by UNU-GTP, GDC and KenGen, at Lake Bogoria and Lake Naivasha, Kenya. (2014). pp. 18.
- Philippe Gamber, Franz LAHAIE, Auxane CHERKAQUI, Régis Farret, Christian Franck, Pascal bicarré. State of knowledge on the risks, impacts and potential nuisances related to deep geothermal energy. Direction of soil and subsoil risks. (2017) pp. 139.
- Pohl, W. Kibarian evolution and metallogeny in Central Africa: a synthesis at the end of I.G.C.P 255, newsletter, (1992). pp. 4-8.

Kawa; Mambo; Kasekete; Syakengwa; Kaizere

Pomerol, C., Lagabriele, Y. and Renard, M. Elements of Geology, 13th Ed. Dunod, Paris, (2006) pp. 764.

Schuman, W. Guide to precious stones, gemstones, ornamental stones, Delachaux and Niestle Neuchatel-Paris, (1976) pp. 128.

Schuman, W. Guides of stones and minerals (rocks, gems and meteorites) Delachaux and Niestle Neuchatel-Paris, (1985). pp. 382.

Sylvain, T. Gold in High-grade Metamorphic Rocks, University of Quebec at Chicoutimi, (2007). pp. 80.

Varlamoff, N. Classification of tin deposits, N.R., XIX-5, Brussel, (1975). pp. 83

WOODTLI. R., THE STRUCTURE OF KILO: Contribution to the study of African ditches Avenue Marniz, 30 BRUSSELS.  
(1956). pp. 129.